

# Observation of antiphase dynamics and harmonic resonance in a modulated dual-wavelength laser

Huibin Chen (陈慧彬)<sup>1,2</sup>, Ge Zhang (张戈)<sup>1</sup>, Wenbin Liao (廖文斌)<sup>1</sup>, Bingxuan Li (李丙轩)<sup>1</sup>, Xiaolei Wang (王小蕾)<sup>1,\*</sup>, and Zhenqiang Chen (陈振强)<sup>3</sup>

<sup>1</sup>Key Laboratory of Optoelectronic Materials Chemistry and Physics, Fujian Institute of Research on the Structure of Matter, Chinese Academy of Sciences, Fuzhou 350002, China

<sup>2</sup>University of Chinese Academy of Sciences, Beijing 100049, China

<sup>3</sup>Institute of Optoelectronic Engineering, Jinan University, Guangzhou 510632, China

\*Corresponding author: wang2022@purdue.edu

Received August 24, 2015; accepted November 6, 2015; posted online December 18, 2015

We observe a nonlinear response of a dual-wavelength Nd:YAG laser when subjected to low-frequency periodic modulations of cavity losses. The modulation frequency is far from the relaxation oscillation frequency. The harmonic resonances of the two laser wavelengths associated with antiphase intensity oscillations are demonstrated and resonances up to the fourth order were observed. For relatively weak modulation, the intensity oscillation frequency of the laser is equal to the modulation frequency. Harmonic resonances occur under a stronger modulation. We find that more harmonic components appear when the modulation frequency is increased. Furthermore, with enhancing the modulation, the dominant frequency of the intensity oscillations of both wavelengths is shifted toward the higher-order harmonic frequency.

OCIS codes: 140.3425, 140.3480, 190.2640.

doi: 10.3788/COL201614.011403.

As a nonlinear dynamical system, a laser with parameter modulation can create a variety of intriguing dynamic effects, including chaos<sup>[1,2]</sup>, antiphase dynamics<sup>[3]</sup>, period doubling<sup>[4,5]</sup>, parametric resonance<sup>[6]</sup>, chaotic phase synchronization<sup>[7]</sup>, etc. The effect of antiphase dynamics in different types of lasers has been studied intensively from the beginning of its discovery by Wiesenfeld *et al.*<sup>[8-14]</sup>. Periodic antiphase oscillations of two orthogonal polarization states have been observed in the Nd-doped fiber laser, and the laser exhibits several nonlinear effects including a period-doubling cascade leading to chaos when the pump modulation is enhanced<sup>[15]</sup>. In this case, the antiphase states correspond to different polarization states, which can be treated as two multimode sets. A nonlinear response can also be observed in a loss-modulated two-mode Fabry-Perot laser<sup>[16]</sup> that shows antiphase dynamics under modulation. In Ref. [16], the laser exhibits notable dynamic behavior when the modulation frequency approaches the relaxation oscillation frequency of the laser, and a simple theoretical model based on the rate equations was successfully developed to describe the antiphase dynamics. The numerical simulations in Ref. [16] also revealed that the harmonic resonance arises when the amplitude of the modulation is increased. In application it has been shown that introducing the small modulation of a parameter can cause an appreciable output modulation to control the intensity instability. For instance, Kang *et al.*<sup>[17]</sup> have demonstrated that the instability in a laser-diode-pumped multimode Nd:YAG laser can be suppressed by the additive modulation of pump current. Using the technique of acoustic wave modulations, Pua *et al.*<sup>[18]</sup> have showed that the irregular intensity

fluctuations in an erbium-doped dual-wavelength fiber laser can be stabilized into periodic orbits that will facilitate the enhancement of the sensing sensitivity. Nevertheless, in most of the studies on modulated lasers, the modulation frequencies have been restricted to the vicinity of the relaxation oscillation frequency of the laser. To our knowledge, features concerning low-frequency modulations have not been reported in dual-wavelength solid-state laser systems.

In this Letter, we report the observation of antiphase dynamics and harmonic resonances in a modulated Nd:YAG laser. The laser operated simultaneously at two wavelengths, 1.319  $\mu\text{m}$  ( $\lambda_1$ ) and 1.338  $\mu\text{m}$  ( $\lambda_2$ ). In our case, compared to true two-mode lasers, each mode was a group of modes around  $\lambda_1$  and  $\lambda_2$  that was actually composed of a large number of individual cavity modes. The antiphase states correspond to the intensity of the two different wavelengths. Two representative types of dynamic phenomena at modulation frequencies of 200 and 500 Hz were chosen for this study. At the modulation frequency of 200 Hz, second harmonic resonances of the two wavelengths associated with antiphase intensity oscillations were demonstrated when the modulation amplitude was increased. In the case of 500 Hz, resonances up to fourth order were observed. Furthermore, with the increasing modulation, the dominant frequency of intensity oscillations of both wavelengths was shifted toward the higher-order harmonic frequency.

Generally, dual-wavelength lasing is governed by both emission cross sections and resonator design in an Nd:YAG laser system<sup>[19]</sup>. By optimizing the reflectivity of the output coupler, lasing can be achieved simultaneously

at two wavelengths. The schematic of the experimental setup is shown in Fig. 1. A diode laser operating at 808 nm was used for side pumping of an Nd:YAG rod (3 mm diameter, 75 mm long, and with 0.7% atomic doping). The maximum pumping intensity was approximately 150 W. The diode bars and the crystal rod were both cooled by recirculating water to keep their temperature at 25°C. The cavity was composed of two plane mirrors, M1 ( $R > 99.9\%$  around 1.3  $\mu\text{m}$ ) and M2 ( $T = 8.1\%$  at  $\lambda_1$  and  $T = 7.6\%$  at  $\lambda_2$ ) that were spaced apart by 105 mm. Both cavity mirrors were also coated with an antireflective coating for 1.064  $\mu\text{m}$  wavelength to suppress this stronger oscillation ( $T = 91.2\%$  at 1.064  $\mu\text{m}$ ).

A small piezoelectric transducer (PZT) ceramic vibrator (resonant impedance:  $\leq 300 \Omega$ , capacitance:  $30000 \pm 30\%$  pF, metal material: brass, diameter: 15 mm, thickness: 0.25 mm), driven by a forcing function generator, was used in our experiment as the modulator. To make sure there was slightly loss modulation caused by minor perturbations, one end of the output coupler mirror was solidly fixed to a mirror mount and the vibrator was directly attached to the other end of the mirror. The loss modulation was introduced in the resonator by slightly tilting the mirror. The output laser intensity was incident upon three beam splitters denoted M3, M4, and M5. Two of the beams passed through gratings adjusted at  $\lambda_1$  and  $\lambda_2$ . The InGaSe photodiode detectors collected the signals and sent them to a multi-input oscilloscope. This setup enabled intensity variation measurement of two separate lasers with different wavelengths as well as their total intensity.

We first considered the operating properties of the dual-wavelength Nd:YAG laser without the modulation. The power ratio between the two wavelengths depended both on the tilt of the coupler mirror and the pumping power<sup>[20,21]</sup>. We did not adjust the output mirror for the maximum efficiency. Instead, the tilt angle of the coupler mirror and the pump current were adjusted for achievement of the comparative intensity of the dual-wavelength emission. Before the deliberate perturbation, we achieved a balanced dual-wavelength emission; the total dual-wavelength lasing power was about 0.85 W at the pumping power of 75 W. The spectral distribution obtained with a spectrophotometer (APE LasScan RS232) is represented in Fig. 2, where the two central wavelengths are at

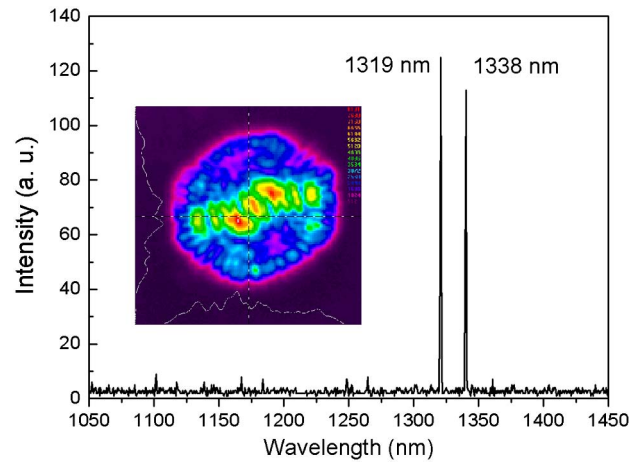


Fig. 2. Measured spectrum of the laser output of two wavelengths and its beam profile.

1.319 and 1.338  $\mu\text{m}$ , respectively. The profile of the two wavelength emission was measured by a pyroelectric camera (Pyrocam III, Ophir Optonics Ltd.) and is given in the insert of Fig. 2. The total laser output is reasonably steady, but the optical signals of both lasing wavelengths showed an instability in the oscilloscope. As shown in Fig. 3(a), the total intensity has a slight fluctuation; however, the intensities of  $\lambda_1$  and  $\lambda_2$  (corresponding to  $I_1$  and  $I_2$ ) exhibit pronounced irregular fluctuations [Figs. 3(b) and 3(c)]. The amplitudes of the two wavelengths were almost inverted with respect to each other; i.e., the maxima of one wavelength tend to coincide with the minima of the other.  $I_1$  and  $I_2$  are essential complementary antiphase synchronizations so that the sum intensity ( $I_1 + I_2$ ) can maintain relative stability. The reason for the above phenomena is that the two emissions share the same upper Stark level, and they will compete for the energy stored in the laser medium. Thus, the feature of mode competition is one of the intrinsic characteristics in dual-wavelength solid laser systems<sup>[18]</sup>.

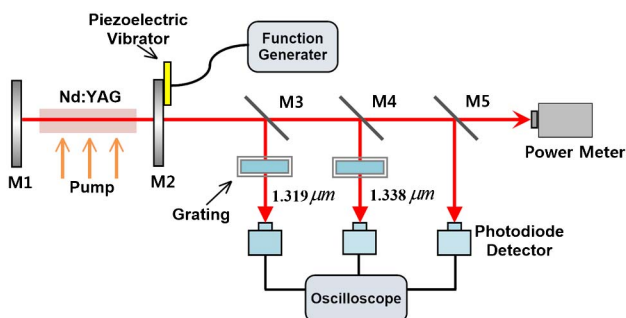


Fig. 1. Schematic of the experiment.

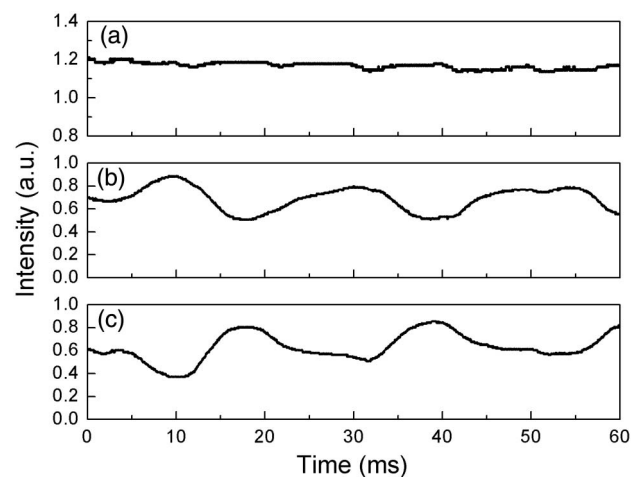


Fig. 3. Temporal characteristics of the intensities of the dual-wavelength laser; (a)  $I_1 + I_2$ , (b)  $I_1$ , and (c)  $I_2$ .

For transient dynamics of a multimode laser, an individual mode shows  $N$  relaxation oscillation frequencies  $f_1 > f_2 > \dots > f_N$  while the total intensity exhibits a unique relaxation oscillation  $f_1$ , just like a single-mode laser, where  $N$  is the number of oscillating modes<sup>[3,22,23]</sup>. In our case, the relaxation oscillation frequency of the laser was estimated to be in the 25–50 kHz range, and each of the wavelengths had approximately 35 longitudinal modes in the laser cavity. Therefore, we concluded that, compared to the relaxation oscillation of the total intensity, there were lower relaxation oscillation frequencies in individual modes that might then be viewed as intrinsic frequencies of the multimode laser system. These frequencies were much lower than the standard relaxation oscillation frequency of the total intensity, and nonlinear effects may appear when the external modulation frequency approaches these low intrinsic frequencies.

After the sinusoidal periodic loss modulation was switched on, the intensity of the vibrator was changed slowly by tuning the generator output voltage. The response frequencies range was nearly from 100 Hz to 1.2 kHz. To show the key dynamics of nonlinear response to the modulation in the laser system, we present here the modulation frequencies of 200 Hz ( $f_{m1}$ ) and 500 Hz ( $f_{m2}$ ) as the examples of illustrations. The laser operation did not have an obvious response to modulation frequencies above 1.2 kHz, probably because the vibrator amplitude was too slight to affect the laser regime in higher modulation frequencies; i.e., it was limited by the piezoelectric vibrator itself.

For small modulating amplitudes, the loss modulation forced the system to oscillate at its own frequency, as shown in Fig. 4. The modulation frequency was  $f_{m1}$  and the generator voltage was 7 V. This aspect of regular intensity oscillation, similar to that of the modulation signal, is usually referred to as a fundamental oscillation. Both wavelengths with pronounced sinusoidal modulations were exactly out of phase with each other [Figs. 4(b) and 4(c)].

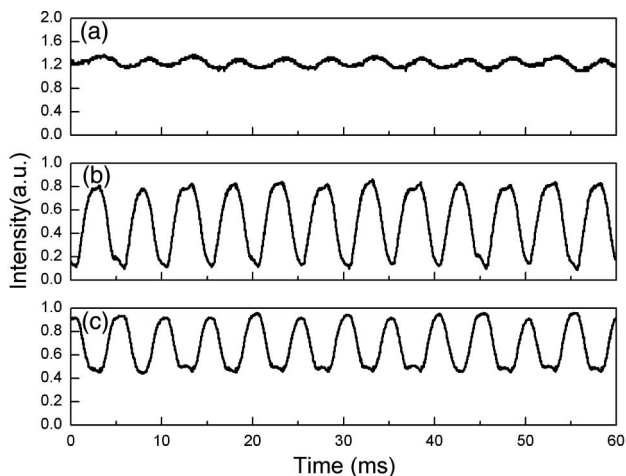


Fig. 4. Temporal characteristics of the intensities of the laser with a 200 Hz modulation and a 7 V generating voltage; (a)  $I_1 + I_2$ , (b)  $I_1$ , and (c)  $I_2$ .

Therefore, the loss introduced on one wavelength will be compensated by the increased gain of the other wavelength, resulting in a small change in the sum intensity.

When the modulation frequency was fixed at  $f_{m1}$ , by progressively increasing the modulation voltage, the component of the second harmonic resonance in the intensity variations of the two wavelengths became gradually stronger. When the modulation amplitude became large enough, the harmonic resonance was dominant over the fundamental oscillation, as shown in Figs. 5(b) and 5(c). In this case, the modulation voltage was up to the highest attainable strength of 20 V. However, the total intensity, exhibiting a slight distortion, showed only the fundamental frequency component [Fig. 5(a)]. Because the total intensity was only the intensity combination of the two wavelengths, it showed that the harmonic oscillation components of two wavelengths interfered destructively, and consequently they were in antiphase. The corresponding power spectra are plotted in Fig. 5(d). The intensities near the zero points are associated with the direct current components of the attenuated laser intensity. These power spectra each have a single prominent peak, one at  $f_{m1}$

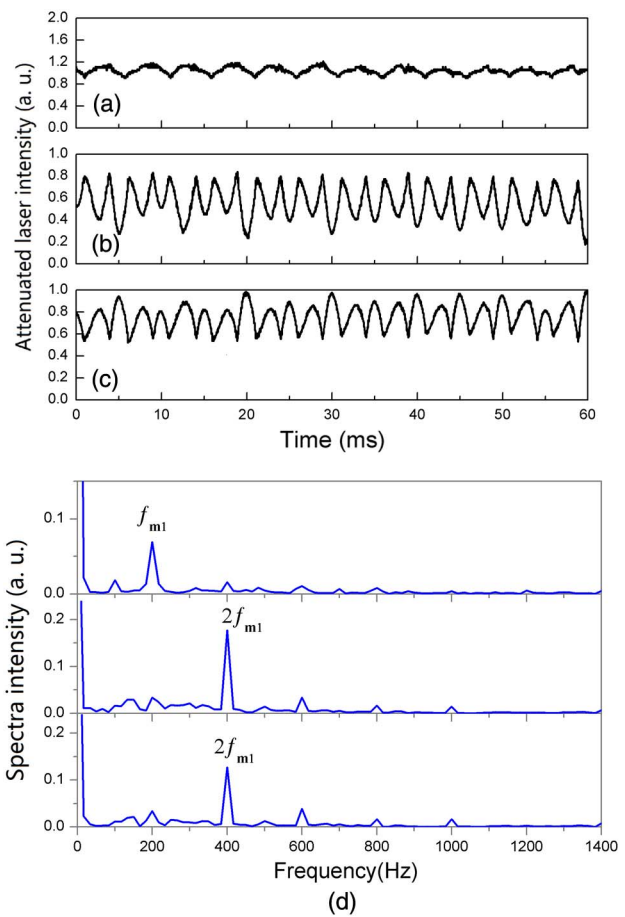


Fig. 5. The response of intensity oscillations of the laser with a 200 Hz modulation and a 20 V generating voltage, indicating second-harmonic resonance; (a)  $I_1 + I_2$ , (b)  $I_1$ , and (c)  $I_2$ . (d) Power spectra corresponding to a, b, and c (from top to bottom).

and two at  $2f_{m1}$ , respectively. We observed that the first peak corresponding to the oscillation at the modulation frequency  $f_{m1}$  exhibited a clear antiphasing property; i.e., the peak at  $2f_{m1}$  for the sum intensity was considerably smaller. This implies the destructive interference between the two lasing.

In the case of  $f_{m2}$ , the response of the sum intensity was similar to the case of  $f_{m1}$ , but the response of the laser in this case exhibited more harmonic components. When the amplitude of the loss modulation was small enough, the response was fundamental oscillation. The second harmonic resonance was observed near 5 V of the modulating voltage. We plot the intensity of the two wavelengths in Figs. 6(a)–6(d). To clarify the low-frequency nonlinear response with increasing modulation amplitude, the corresponding power spectra of the intensity oscillations of two wavelengths are plotted in Fig. 7, where the evolution of the oscillation frequency corresponds to  $I_1$  and  $I_2$ , respectively. It is apparent that higher-order harmonics arise with enhancing of the modulation. When increasing the strength of the modulation, the dominant frequency of the intensity oscillations of the two wavelengths switched from  $f_{m2}$  to  $2f_{m2}$ ,  $3f_{m2}$ , and then to  $4f_{m2}$ . These correspond to the fundamental oscillation frequency, frequency doubling, tripling, and quadrupling. In other words, higher harmonic oscillations can be excited as modulation enhancement, and the dominant harmonic component depends crucially on the modulation amplitude. As a result, by varying the periodically modulating loss magnitude, the dual-wavelength laser tends to operate in a macrotemporal pulsed regime, with an adjustable period in the range of milliseconds.

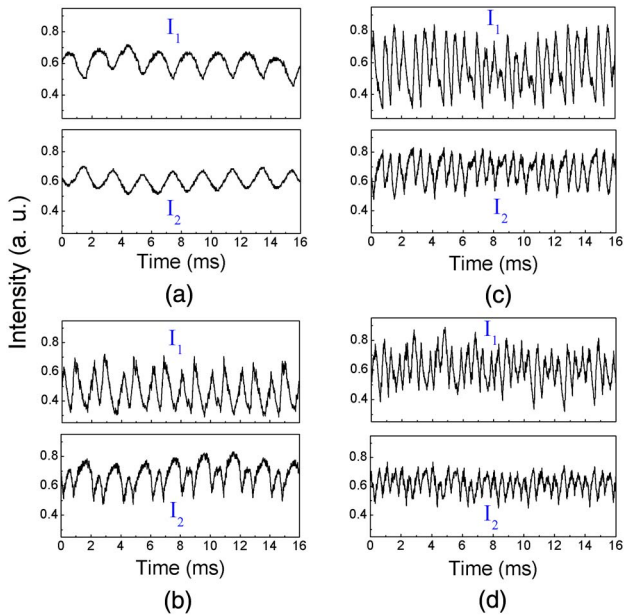


Fig. 6. Experimental time evolution of the two separate wavelengths with a 500 Hz modulation. The corresponding voltage modulations are (a) 1, (b) 5, (c) 5.5, and (d) 8 V. Note that, for increasing modulating amplitudes, the system exhibits antiphase dynamics within the higher-order harmonic resonance.

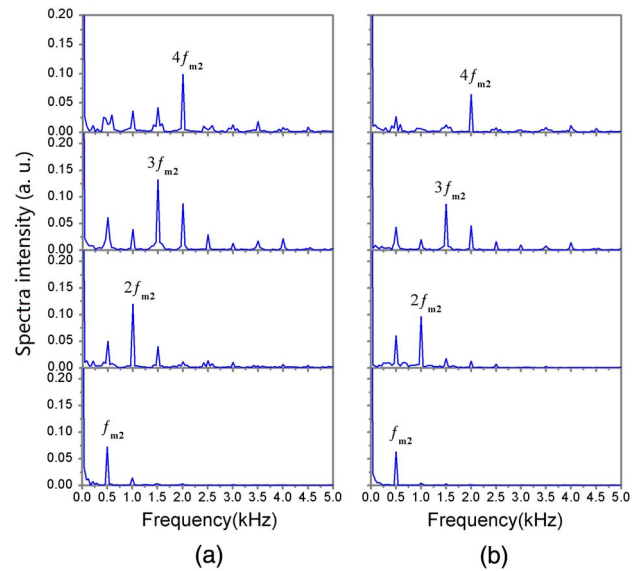


Fig. 7. Power spectra corresponding to Fig. 6; (a) refers to  $I_1$  and (b) refers to  $I_2$ . The modulating voltage is growing from bottom to top.

Among the response frequencies, we found that the higher harmonic components came along with the higher modulation frequencies for the same modulating intensity. The second harmonic component was obvious in the modulation frequency of 200 Hz, and the highest fourth harmonic was observed in the range of 0.5–1.2 kHz. We also found that this behavior was strongly affected by the input pumping power. In the case of a given perturbation, a higher input pumping power can force the intensity oscillation of both wavelengths to oscillate at a higher-harmonic frequency. This is because of the stronger competition between the two lasing wavelengths for population inversions in the active medium of the laser, which favors the appearance of harmonic resonances at multiples of the modulation frequency.

In conclusion, we discover a new nonlinear response in a modulated dual-wavelength Nd:YAG laser, including antiphase dynamics and harmonic resonance. Nonlinear effects of frequency doubling, frequency tripling, and frequency quadrupling of the laser intensity oscillation under a low-frequency modulation are demonstrated for the first time to our knowledge. We find that the higher-order harmonic resonance is more likely to occur when the laser is subjected to a large amplitude modulation. The antiphase state between the two different wavelengths is found to be within higher-order harmonic resonances.

This work was supported by the Natural Science Foundation of Fujian Province (No. 2013J05106) and the Fujian High Technology Research and Development Program (No. 2012H0046).

## References

1. W. Klische, H. R. Telle, and C. O. Weiss, *Opt. Lett.* **9**, 561 (1984).
2. S. Yan, *Chin. Opt. Lett.* **13**, 040401 (2015).

3. K. Otsuka, P. Mandel, M. Georgiou, and C. Etrich, *Jpn. J. Appl. Phys.* **32**, L318 (1993).
4. W. F. Ngai and H. F. Liu, *Appl. Phys. Lett.* **62**, 2611 (1993).
5. M. Ma, Z. Hu, P. Xu, W. Wang, and Y. Hu, *Chin. Opt. Lett.* **12**, 081403 (2014).
6. K. Otsuka, D. Pieroux, J. Y. Wang, and P. Mandel, *Opt. Lett.* **22**, 516 (1997).
7. A. Ahlborn and U. Parlitz, *Opt. Lett.* **34**, 2754 (2009).
8. K. Wiesenfeld, C. Bracicowski, G. James, and R. Roy, *Phys. Rev. Lett.* **65**, 1749 (1990).
9. K. Otsuka, P. Mandel, S. Bielawski, D. Derozier, and P. Glorieux, *Phys. Rev. A* **46**, 1692 (1992).
10. D. Y. Tang and N. R. Heckenberg, *Phys. Rev. A* **56**, 1050 (1997).
11. D. Y. Tang, R. Dykstra, and N. R. Heckenberg, *Opt. Commun.* **126**, 318 (1996).
12. S. Osborne, A. Amann, K. Buckley, G. Ryan, S. P. Hegarty, G. Huyet, and S. O. Brien, *Phys. Rev. A* **79**, 023834 (2009).
13. A. M. Yacomotti, L. Furfaro, X. Hachair, F. Pedaci, M. Giudici, J. Tredicce, J. Javaloyes, S. Balle, E. A. Viktorov, and P. Mandel, *Phys. Rev. A* **69**, 053816 (2004).
14. J. Dong, A. Shirakawa, and K. I. Ueda, *Eur. Phys. J. D* **39**, 101 (2005).
15. S. Bielawski, D. Derozier, and P. Glorieux, *Phys. Rev. A* **46**, 2811 (1992).
16. B. A. Nguyen and P. Mandel, *Opt. Commun.* **112**, 235 (1994).
17. M. H. Kang, K. M. Cho, C. M. Kim, S. K. Gil, and J. C. Lee, *J. Opt. Soc. Am. B* **15**, 2410 (1998).
18. C. H. Pua, H. Ahmad, S. Harun, and R. M. De La Rue, *IEEE J. Quantum Electron.* **48**, 1499 (2012).
19. H. Shen and H. Su, *J. Appl. Phys.* **86**, 6647 (1999).
20. H. Zhu, G. Zhang, C. Huang, Y. Wei, L. Huang, A. Li, and Z. Chen, *Appl. Phys. B* **90**, 451 (2008).
21. F. Pallas, E. Herault, J. Zhou, J. F. Roux, and G. Vitrant, *Appl. Phys. Lett.* **99**, 241113 (2011).
22. P. Mandel, M. Georgiou, K. Otsuka, and D. Pieroux, *Opt. Commun.* **100**, 341 (1993).
23. D. Pieroux, T. Erneux, and P. Mandel, *Phys. Rev. A* **54**, 3409 (1996).